Journal Pre-proof

Development and primary characterization of a human thyroid organoid *in vitro* model for thyroid metabolism investigation

Sofia Cristiani, Andrea Bertolini, Vittoria Carnicelli, Lucia Contu, Valentina Vitelli, Alessandro Saba, Federica Saponaro, Grazia Chiellini, Antonietta Raffaella Maria Sabbatini, Maria Anita Giambelluca, Paola Lenzi, Francesco Fornai, Leonardo Rossi, Gabriele Materazzi, Carlo Enrico Ambrosini, Grazia Rutigliano, Riccardo Zucchi, Ranieri Bizzarri, Sandra Ghelardoni

PII: S0303-7207(24)00233-8

DOI: https://doi.org/10.1016/j.mce.2024.112377

Reference: MCE 112377

To appear in: *Molecular and Cellular Endocrinology*

Received Date: 10 June 2024

Revised Date: 20 August 2024

Accepted Date: 23 September 2024

Please cite this article as: Cristiani, S., Bertolini, A., Carnicelli, V., Contu, L., Vitelli, V., Saba, A., Saponaro, F., Chiellini, G., Sabbatini, A.R.M., Giambelluca, M.A., Lenzi, P., Fornai, F., Rossi, L., Materazzi, G., Ambrosini, C.E., Rutigliano, G., Zucchi, R., Bizzarri, R., Ghelardoni, S., Development and primary characterization of a human thyroid organoid *in vitro* model for thyroid metabolism investigation, *Molecular and Cellular Endocrinology*, https://doi.org/10.1016/j.mce.2024.112377.

This is a PDF file of an article that has undergone enhancements after acceptance, such as the addition of a cover page and metadata, and formatting for readability, but it is not yet the definitive version of record. This version will undergo additional copyediting, typesetting and review before it is published in its final form, but we are providing this version to give early visibility of the article. Please note that, during the production process, errors may be discovered which could affect the content, and all legal disclaimers that apply to the journal pertain.

© 2024 Published by Elsevier B.V.

Graphical Abstract

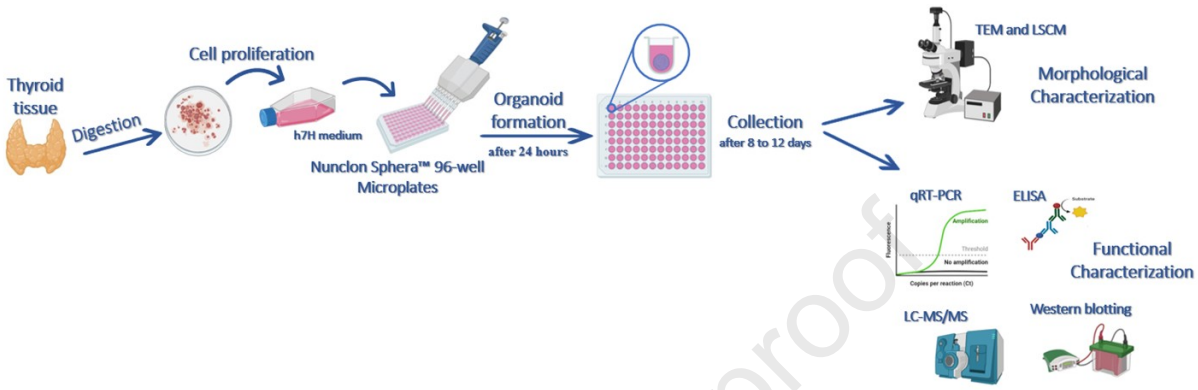

Journal Pre-proof

Development and primary characterization of a human thyroid organoid *in vitro* model for thyroid metabolism investigation

Sofia Cristiani[1†], Andrea Bertolini[1†], Vittoria Carnicelli[1], Lucia Contu[1], Valentina Vitelli[1], Alessandro Saba[1], Federica Saponaro[1], Grazia Chiellini[1], Antonietta Raffaella Maria Sabbatini[1], Maria Anita Giambelluca[2], Paola Lenzi[2], Francesco Fornai[2,3], Leonardo Rossi[4], Gabriele Materazzi[4], Carlo Enrico Ambrosini[4], Grazia Rutigliano[1], Riccardo Zucchi[1], Ranieri Bizzarri[1], Sandra Ghelardoni[1]*

[1] *Department of Surgical, Medical and Molecular Pathology and Critical Care Area, University of Pisa, via Roma 55, 56126 Pisa, Italy.*

[2] *Department of Translational Research and New Technologies in Medicine and Surgery, University of Pisa, via Roma 55, 56126 Pisa, Italy.*

[3] *Istituto di Ricovero e Cura a Carattere Scientifico (IRCCS), Neuromed, 86077 Pozzili, Italy*

[4] *Endocrine Surgery Unit, University Hospital of Pisa, Pisa, Italy*

** Corresponding author, Department of Surgical, Medical and Molecular Pathology and Critical Care Area, University of Pisa, via Roma 55, 56126 Pisa, Italy, sandra.ghelardoni@unipi.it*

† The authors contributed equally to this manuscript

Abstract

A 3D thyroid model was developed to address the limitations of 2D cultures and study the effects of compounds like 3-MNT on dehalogenase 1 (IYD) and metabolic activity. Morphology was assessed by TEM, and the expression of tissue-specific genes (*TPO*, *TSHR*, *PAX8*, *TTF-1*, *NIS*, *IYD*, *TG*) and metabolic features were analyzed using qRT-PCR, immunofluorescence, western blotting, ELISA, and LC-MS/MS, with and without TSH stimulus and 3-MNT treatment. Confocal and TEM analyses confirmed a follicle-like 3D structure. Expression of *TPO*, *NIS*, *TG*, *TSH*, and *PAX* markers was significantly higher ($p < 0.05$) in 3D versus 2D cultures, and ELISA showed increased TG protein production. 3-MNT treatment inhibited IYD activity, indicated by increased MIT and DIT in the media, and significantly altered ($p < 0.05$) *NIS*, *TG*, *IYD*, *TSHR*, and *TPO* expression. These findings suggest 3D thyroid cultures closely replicate tissue traits and functionality, providing a valuable tool for thyroid research.

Keywords: thyroid; organoid; TSH; IYD; 3-MNT; disruptors.

Journal Pre-proof

1. Introduction

The thyroid gland regulates metabolism by producing thyroid hormones (TH), mainly T4 (Thyroxine) and T3 (Triiodothyronine) (Gereben et al., 2015; Luongo et al., 2019). T4 acts as a prohormone, converting into active T3 in peripheral tissues via deiodinase enzyme (DIOs) (Bianco and Kim, 2006). The Hypothalamic-Pituitary-Thyroid axis (HPT) maintains TH levels. Thyrotropin-Releasing Factor (TRH) stimulates pituitary Thyroid Stimulating hormone (TSH) release, which triggers TH synthesis (Estrada et al., 2014; Fekete and Lechan, 2014) within thyroid follicles. Here, thyroglobulin (TG), containing tyrosine residues, facilitates iodine attachment (Citterio et al., 2019). The sodium-iodide symporter (NIS) enables iodine uptake into thyroid cells (Wright and Turk, 2004). TSH regulates TG endocytosis via the TSH receptor (TSHR) and iodide efflux through channels like pendrin (Gillam et al., 2004; Kogai et al., 1997; Ohno et al., 1999; Portulano et al., 2014). Thyroid peroxidase (TPO) catalyzes iodination and coupling of iodotyrosines, MIT and DIT, on TG to synthesize TH. The coupling MIT and DIT leads to the formation of T4 and T3 (Ameziane-El-Hassani et al., 2005; Belforte et al., 2015; Carvalho and Dupuy, 2013; Godlewska et al., 2014; Yokoyama and Taurog, 1988). TSH stimulation leads to endocytosis of newly TH bound to TG into thyrocytes, where lysosomal enzymes release T3 and T4. Uncoupled MIT and DIT are enzymatically deiodinated by iodotyrosine dehalogenase (DEHAL1/IYD), enabling their reuse in TH biosynthesis (Gnidehou et al., 2004). Transcription factors PAX8 (Paired Box-8) and TTF-1 (Thyroid Transcription Factor-1) are responsible, together with all the aforementioned actors, for the development and correct functioning of the thyroid gland (Fabbro et al., 1994).

In vitro models offer a platform for dissecting cellular pathways and responses, facilitating the exploration of thyroid physiology and pathophysiology (Samimi et al., 2021). Conventional two-dimensional (2D) cell culture systems have long served as fundamental tools for understanding and investigating cellular and molecular biology, including thyroid metabolism. Yet, their simplified nature often fails to recapitulate the physiological complexity observed *in vivo*, where cells exist in a complex 3D microenvironment with organized interactions among neighboring cells and the extracellular matrix (ECM), crucial for differentiation, proliferation, and function. 2D cultures lack nutrients, oxygen gradients and structural complexity of the tissue, resulting in altered cell morphology and function, and forming unnatural monolayers that affect signaling pathways, gene expression, and behavior. Furthermore, 2D cultures do not replicate the mechanical forces experienced by cells *in vivo*, such as tension, compression, and shear forces, resulting in differences in cell signaling and physiology. The advent of three-dimensional (3D) organoid models has revolutionized the field by providing a more physiologically relevant environment that better recapitulates tissue architecture and function (Samimi et al., 2021). First studies on thyroid organoids were carried out by differentiating mouse embryonic or pluripotent stem cells into thyroid follicular cells in vitro, generating functional thyroid tissue (Antonica et al., 2012; Kurmann et al., 2015; Longmire et al., 2012; Shankaran et al., 2021) till the use of human embryonic stem cell or primary thyrocytes (Deisenroth et al., 2020; Romitti et al., 2022; Wang et al., 2016). The transition from 2D to 3D culture systems represents a paradigm shift, offering researchers a more accurate representation of *in vivo* conditions and enhancing the translational potential of *in vitro* findings (Lelièvre et al., 2017). Organoids, self-organizing 3D structures derived from stem cells or tissue

progenitors, have gained prominence as valuable tools in various fields of biomedical research (Edmondson et al., 2014). Their ability to mimic organ-specific architecture and function makes them particularly suitable for studying complex biological mechanisms, including endocrine function (Dalir Abdolahinia and Han, 2023; Hwang et al., 2021; Jubelin et al., 2022). The utilization of organoids in *in vitro* assays presents unprecedented opportunities for investigating thyroid metabolism with enhanced fidelity and relevance. Moreover, this approach aligns with the scientific 3R principles (Replacement, Reduction, Refinement), promoting ethical use of different biological matrices in research, maximizing the possible scientific outcomes, advancing our understanding of thyroid physiology in a more humane and efficient manner (Tannenbaum and Bennett, 2015). Thyroid alterations may occur during physiological processes such as pregnancy as well as specific disorders including tumor malignancy. Very often thyroid dysfunctions are triggered by exogenous disruptors, which interfere with the regular production of hormones, also known as endocrine disruptors (EDs). The rise in endocrine disorders and the widespread presence of endocrine-disrupting chemicals highlight the need for robust models to assess their impact on thyroid function. Exposure to EDs has been linked to an increase in neurodevelopmental disorders and a decline in average IQ (Asawasinsopon et al., 2006; Chevrier et al., 2008; de Escobar et al., 2007; Haddow et al., 1999; Hetzel, 2000; Lopez-Espinosa et al., 2009; Román et al., 2013; Zimmermann et al., 2008). Some EDs may inhibit IYD, leading to iodine loss in urine, mimicking iodine deficiency, and alter the cellular redox and metabolic state (González-Guerrero et al., 2023; Shareef et al., 2023). Organoids offer a promising approach to understanding endocrine disruption mechanisms, assessing health risks from environmental contaminants, and guiding regulatory efforts to protect public health. Given that a significant part of worldwide population will experience a thyroid disorder during their lifetime (Sewell and Lin, 2014), the need to develop thyroid organoid models for finding appropriate and specific treatments becomes even more critical.

In this study, we focused on the development and primary characterization of a human thyroid organoid *in vitro* model tailored with the aim of evaluating a 3D model for investigating thyroid metabolism and observing the effects of compounds which can interfere in recycling iodine. Morphology was characterized by confocal and transmission electron microscopy (TEM). The expression of functional thyroid markers and metabolic features, with and without TSH stimulus or upon treatment with 3-mono-L-nitro tyrosine (3-MNT), a competitive inhibitor of IYD, were examined by quantitative reverse transcription real time polymerase chain reaction (qRT-PCR), immunocytofluorescent staining, western blotting and ELISA. MIT/DIT release upon 3-MNT treatment as well as TH production were monitored using tandem mass spectrometry coupled to high performance liquid chromatography (LC-MS/MS).

2. Materials and methods

2.1 Chemicals

Unless otherwise specified, all reagents were from Sigma Aldrich-Merck (Merck KGaA, Darmstadt, Germany). Reagents for 2D or 3D cell cultures were from Gibco™, Thermo

Scientific™, Waltham, MA, USA. Solvents for HPLC-MS/MS measurements were HPLC grade, and the other chemicals were reagent grade. $^{13}C_9$-MIT and $^{13}C_9$-DIT were kindly provided by Prof. Alireza Mani (University College of London, UK), since they were not commercially available.

2.2 2D cell culture and 3D organoid formation

Non-tumorous thyroid samples were obtained from healthy donors (University Hospital of Pisa, Italy) during routine thyroidectomy procedures in individuals at Endocrine Surgery Unit. All participants signed the informed consent and advance directives (according to Law No. 219/2017). To allow cell isolation, the samples were minced and digested through collagenase IV (1 mg/mL and 3 mM $CaCl_2$) at 37 °C and 5% CO_2 for 2 hours. The isolated cells were seeded into flasks with Humanized 7 homeostatic additives (h7H) medium (Bravo et al., 2013) supplemented with standard 5% Newborn Calf Serum (NCS), 5% Fetal Bovine Serum (FBS), and 2% Penicillin-Streptomycin , and incubated at 37 °C and 5% CO_2 in a humidified chamber, until 70- 80 % of confluence was reached. Then, confluent primary thyrocytes were detached (passage 0) with TrypLE™ Express Enzyme, no phenol red and plated in round-bottomed Nunclon Sphera™ 96-well Microplates in h7H and 3% Geltrex™, 37 °C and 5% CO_2, at a density of 10000 cells/well to maintain uniform size among cell aggregates that were collected after 8 to 12 days from seeding, without further passages. All experiments utilized cells at passage 0 (P0) or 1 (P1) for 2D, unless otherwise indicated.

2.2 3D Organoid treatment

On day 8, the following treatments were performed for 4 days on organoids: no TSH (control), and TSH (2 mU/mL, from bovine pituitary); 0.01 µM 3-MNT, 1 µM 3-MNT, 100 µM 3-MNT, or vehicle (0.05 mM NaOH), all in TSH condition. At the end of each treatment, organoids were collected for morphological and functional characterization experiments as depicted in the following paragraphs. The experiment was repeated on three donors.

2.3 Human Thyroglobulin (TG) Enzyme-linked immunosorbent assay (ELISA)

Human Thyroglobulin ELISA (Human Thyroglobulin ELISA kit #EHTG Thermo Scientific™) was performed following the manufacturer's protocol in the cell culture effluent. Analysis was conducted on exhausted h7H medium collected from both 2D and 3D cultures derived from a single donor, after 4 days of incubation with or without 3-MNT or vehicle. Data collection was conducted on a microplate reader at 450 nm (Bio-Rad, Hercules, CA, USA).

2.4 Immunofluorescence assay

Both 2D and 3D thyroid cultures were fixed in 4% Paraformaldehyde (PFA) in PBS for 30 minutes at room temperature (RT). Organoids were maintained in suspension, rinsed three

times in 0.1% TBST wash buffer and permeabilized with 0.5% TBST buffer for 30 minutes. After a wash with 0.1% TBST, organoids were incubated in blocking buffer (0.1% TBST plus 2% w/v BSA) for 1 hour at RT and, thus, incubated with the primary antibody (Table S1) overnight at 4 °C, and then with the corresponding secondary antibody (Table S2). Organoids were mounted on microscope slides with DAPI Mounting Medium (Abcam). Images were acquired using a laser scanning confocal microscope (Nikon, Eclipse, Ti) Amstelveen, Netherlands)) and processed using ImageJ Programme (Sun-Java, National Institutes of Health, USA). For 2D culture immunolabelling, cells were permeabilized with 0.1% Triton X-100 in PBS for 20 minutes, then incubated with the blocking solution (2% BSA) for 45 minutes at RT. 2D systems were incubated with the same primary antibodies used for the 3D cultures, except for α-tubulin (Table S1) primary antibody which replaced Phalloidin antibody to amplify the signal by indirect immunolabelling and then with the corresponding secondary antibodies (Alexa Fluor™ 488, 1:400, goat anti-mouse ab150113, Abcam, used against mouse α-tubulin primary antibody).

2.5 Gene expression

For gene expression comparison of 2D and 3D cultures total RNA was isolated from 1.8 x 10^6 cells at passages P0 and P1 and from 16 pooled organoids collected within 12 days from seeding. RNA extraction was performed with Direct Zol RNA Microprep Kit (Zymo Research, USA), following company protocol. The kit on-column DNase incubation step was included. RNA was quantified with Qubit Fluorometer (Thermo Fisher Scientific) in association with Quanti It RNA BR Kit (Thermo Fisher Scientific). Total RNA (100 to 500 ng) was retrotranscribed into cDNA by using iScript gDNA Clear cDNA Synthesis Kit (Bio-Rad) as manual protocol indications.

Relative quantity of gene transcripts was measured by RT-PCR on cDNA samples using SsoAdvanced Universal SybrGreen Master Mix (BioRad) on a CFX Connect RT-PCR Detection System (Bio-Rad). All reactions were conducted in duplicate. Negative control of retro-transcription was performed to exclude any interference from residual genomic DNA contamination. PCR Primer Assay (Bio-Rad) for thyroid markers genes were indicated in supplementary materials, Table 1. Samples were analyzed by the $2^{-\Delta\Delta Ct}$ method as described by Livak and Schmittgen (Livak and Schmittgen, 2001). The relative expression of the target genes was normalized to the level of *GAPDH*.

2.6 TEM evaluation

For TEM analysis, human thyroid organoids were rinsed in PBS, and fixed in a solution of 2.0% paraformaldehyde and 0.1% glutaraldehyde in 0.1 M PBS (pH 7.4) for 90 minutes at 4 °C. After washing in PBS 0.1 M, samples were post-fixed in 1% osmium tetroxide (OsO4, Agar Scientific Ltd, Stansted, Essex) for 1 hour at 4 °C. Samples were then dehydrated in increasing ethanol solutions (50%, 70%, 90% and 95% for 5 minutes; and 100% for 60 minutes), and finally, they were embedded in Epoxy resin. Semi-thin slices (about 1 μm thick) were cut by ultramicrotome (Leica Microsystems, Leica Microsystems, Wetzlar, Germany),

and they were stained with toluidine blue and observed at light microscopy (Nikon, Tokyo, Japan). Semi-thin slices served as a guide to cut specific ultra-thin slices (70–90 nm thick) to combine light and electron microscopy analysis of specific micro-areas. Ultra-thin slices were counterstained with uranyl acetate and lead citrate and were observed at Jeol JEM SX100 electron-microscope (Jeol, Tokyo, Japan).

2.7 Protein expression analysis

To observe the presence of IYD protein in the different cell cultures, qualitative IYD expression analysis was assessed in 2D thyroid cell cultures and organoids (thyroid tissue extracts were used as positive controls), which were collected after 8 days from seeding. Cells or pools of 32 organoids were extracted in ice-cold extraction buffer as elsewhere described (Bandini et al., 2022). Thyroid samples were homogenized using a Teflon-glass homogenizer in ice-cold buffer for tissue extraction (Tissue extraction reagent, Thermo-Fischer Scientific, supplemented with 1 mM phenylmethanesulfonyl fluoride and protease inhibitor cocktail) and then centrifuged to collect supernatant. Protein concentration was determined by Protein Assay Dye Reagent Concentrate (Biorad). To perform western blotting, proteins were resolved by SDS-PAGE (4-20% acrylamide separating gel, Biorad) and transferred onto a PVDF membrane (Biorad), which was incubated with primary antibody (Table S4) and then with anti-rabbit secondary antibody (Table S4). For neutralization, antibody for IYD was incubated overnight at 4 °C with excess of blocking peptide (Table S4). Immunoblots were visualized by means of a chemiluminescence reaction by ImageLab™ Software under a luminescent image analyzer (Chemidoc XSR+, Bio-Rad)

2.8 Measurement of cell viability

The cytotoxic effect of 3-MNT on primary thyrocytes was determined using a 3-(4,5-Dimethylthiazol-2-yl)-2,5-diphenyltetrazolium bromide (MTT) assay, according to manufacturer's specifications. MTT assay was performed on cells treated with increasing concentrations of 3-MNT, from 0.05 µM up to 200 µM, or an equal volume of 0.05 mM NaOH as control for 24 hours. Absorbance was measured at 570 nm on a microplate spectrophotometer (Bio-Rad). Afterwards three concentrations of this IYD inhibitor were chosen for 3-MNT treatment experiments.

2.9 LC-MS/MS Media sample analysis

Each condition (inhibitor 3-MNT 0.01 µM, 1 µM and 100 µM, and the vehicle 0.05 mM NaOH; TSH 2 mU/mL and no further addition of TSH) was performed on 16 different organoids (therefore 16 media wells), and the media from each of the 16 wells were collected for analysis. To minimize variability in the evaluation of tyrosines and thyronines concentrations within the various wells, media pools were created by taking the same volume (6.25 µL) from each well (for each treatment) to reach a final volume of 100 µL. To appreciate tyrosines and thyronines production differences in organoids culture media, with and without a TSH stimulus to study the active organoid metabolism (2 mU/mL for 4 days), media were collected and analyzed for T3, T4, MIT and DIT concentrations as well.

To each 100 µL of media sample or pool, 10 µL of a 100 ng/mL mixture of labelled internal standards, containing $^{13}C_9$-MIT, $^{13}C_9$-DIT, $^{13}C_6$-T3 and $^{13}C_6$-T4 were added. The samples were then processed and analyzed as previously described (Borsò et al., 2022; González-Guerrero et al., 2023; Shareef et al., 2023). Since the method was originally optimized on plasma/serum and urines (Borsò et al., 2022; González-Guerrero et al., 2023; Shareef et al., 2023), the recovery rates (%) of analytes and the matrix effect in the media analyzed samples were calculated as reported by Matuszewski et al. 2003 (Matuszewski et al., 2003). Recovery was evaluated by comparing the peak areas of isotope labelled internal standards analytes-analogues added to the media before and after the extraction procedure, while the estimation of matrix effect was performed comparing the peak areas of the isotope labelled internal standards analytes-analogues added to water (A) and media (B) previously subjected to the extraction process [(B/A) x 100].

2.10 Statistical Analysis

Results are expressed as the mean ± S.E.M. Differences between two groups were analyzed by Student's t-test, while differences between multiple groups were analyzed by one-way or two-way ANOVA as detailed for each figure. In the experiments aimed at determining differences between groups, Tukey's post hoc comparison test was applied. The threshold of statistical significance was set at $P < 0.05$. GraphPad Prism version 9.0 for Windows (GraphPad Software, San Diego, CA, USA) was used for data processing and statistical analysis.

3. Results

3.1 Thyroid 3D culture formation

Organoids derived from human non-tumorous primary thyrocytes were collected after 8 to 12 days following cell seeding. In Figure 1.A it is possible to see the formation and spatial organization processes of the 3D cultures from confluent primary thyrocyte seeding up (Figure 1.A1-2) to the collection of organoids (Figure 1.A 3-5). Each well of the 96-well microplates hosted just a single organoid whose diameter was about 200 µm. No numerous smaller organoids with variable diameters were found in the same well. The spheroidal morphology and 200 µm diameter were two features preserved among organoids formed in different wells within the same experimental microplate.

3.2 Immunofluorescence characterization

The morphology and positivity for thyroid markers of both 2D and 3D culture systems were investigated by immunofluorescent staining and laser scanning confocal microscopy (LSCM) visualization. As shown in Figure 1.B, monolayer P0 primary thyrocytes preserved the identity of the original organ by expressing functional thyroid marker IYD, TSHR and TTF-1. However, the polarized structure typical of follicular cells, defined by a basolateral membrane and an apical membrane displaying microvilli (Arvan et al., 1997), started to be less visible due to progressive reduction in thyrocyte phenotype induced by the monolayer culture

condition. Similarly, the 3D cultures (Figure 1, C) proved to maintain positive labelling for the same functional thyroid markers, IYD, TSHR and TTF-1. to provide a deeper investigation of 3D culture structure, we proceeded with a morphological characterization by TEM microscopy.

3.3 TEM morphological characterization

To analyse the morphology of human thyroid organoids we used light microscopy on semi-thin slices stained with toluidine blue and transmission electron microscopy. This approach allows a progressive increase in magnification in order to detail the architecture of the samples. Toluidine blue staining of resin embedded semi-thin sections provides high quality and clear detailed images of structures as reported in representative Figure 2A. The thyroid organoid shows a central cavity delimited by epithelial cells. The central cavity is well evident in ultrathin sections (Figure 2.A1-A2). The cell apical surface, that protrudes in the cavity, possesses short and sparse microvilli (Figure 2.A3). Droplets, containing a poorly electrodense material similar to the colloid, are located in sub-apical cytoplasm (Figure 2.A4).
Figure 2.B1 shows two adjacent cells with junctional complexes at their apical lateral membrane. Epithelial cells possess well developed Golgi apparatus and rough endoplasmic reticulum (RER), in particular RER is located in the nuclear region and its cisternae are markedly dilated (Figure 2.B2-B3). Several mitochondria are dispersed in the cytoplasm (Figure 2.B2-B4). Lysosomes are large in diameter, and they appear in different forms (Figure 2.B4). Moreover, basal body of primary cilium (PC) was observed in epithelial cells (Figure 2.B1).

3.4 Expression of functional markers in thyrocyte preparations

3.4.1 Genetic analysis

We evaluated the expression of thyroid differentiation markers genes *PAX8* and *NKX2-1*/ *TTF-1* and four thyroid functional marker genes (*IYD*, *TG*, *TSHR*, *TPO*, *NIS*) from both monolayer and 3D cultures. As reported in Figure 3.A, the relative expression of each gene was significantly higher in the 3D system than in the two 2D systems. Particularly, the expressions of *IYD* (fold-change: 24.15; ***$p<0.001$), *TG* (fold change: 3.55; *$p<0.05$), *TSHR* (fold change: 6.13; **$p<0.01$), *TPO* (fold change: 9.52; *$p<0.05$), *NIS* (fold change: 179.72; *$p<0.05$) and transcription factor *PAX8* (fold change: 216.52; **$p<0.01$) and *TTF-1* (fold change: 9.93; *$p<0.05$) genes were significantly increased in the organoid models, supporting the preservation of thyroid differentiation identity and functionality in organoids. These results indicate that the transcriptional regulation of thyrocyte differentiation marker genes is remarkably influenced by the organoid format which maintains and promotes a differentiated thyroid phenotype.

3.4.2 Western Blotting analysis

As shown in Figure 3.B (B1-B2), 2D cell lysates or tissue extracts, the latter used as positive control (C+), incubated with the anti IYD antibody, showed several bands but only the

appearance of band between 25 and 37 kDa was prevented by peptide neutralization. In 2D cell lysates (Figure 3.B1), IYD was detected only at seeding passage (P0) but not at the subsequent passages, corroborating the loss of phenotype characterization observed by immunofluorescence analysis as described above. IYD protein expression was also detectable in organoids cultured in Nunclon plates for 8-12 days, (Figure 3.B4), indicating a continuous production of the enzyme in the 3D system opposed to the 2D system. To verify the presence of proteins in extracts, the same blots were stripped and then probed with α-actin (Figure 3. B3 and B5, for B1 and B4 respectively).

3.4.3 TG production analysis by ELISA assay

Monitoring TG concentration in 2D, namely at P0 and P1 passages, and 3D models is a useful tool to evaluate if TH biosynthesis activity is preserved. As depicted in Figure 3.C, the 3D system produced a significantly greater amount (TG: 2066 ± 57 ng/mL, ****$p < 0.0001$) of thyroglobulin than the 2D monolayer (TG: P0, 809 ± 122 ng/mL; P1, 978± 72 ng/mL), in normal h7H medium culture condition, revealing how significantly relevant 3D spatial organization could be for primary thyrocytes to maintain the production of TH precursor.

3.5 Effects of TSH stimulus on thyroid-like follicle metabolism

3.5.1 TG production

To qualitatively evaluate the responsiveness to TSH stimulation on the production of TG, which is physiologically regulated by the HPT axis, 3D cultures were incubated with or without 2 mU/mL TSH for 4 days after seeding (from day 8 to day 12) and TG concentration was assessed in culture medium. As shown in Figure 4.A, if compared to the no TSH condition (362 ± 51 ng/mL), TSH treatment led to a slight increase in TG (422 ± 75 ng/mL), although not statistically significant.

3.5.2 Gene expression analysis

We investigated the effect of adding an extra amount of TSH hormone (2 mU/mL) to h7H medium for 4 days on TH biosynthesis gene expression, as opposed to TSH starvation, which consisted in no further addition of the hormone to the media. Despite an overall increase in *IYD* (fold-change: 2.40), *TG* (fold-change: 2.31), *TSHR* (fold-change: 1.79) and *TPO* (fold-change: 2.02) gene expression levels (Figure 4.B), we found no significant difference between the two experimental conditions, potentially due to the already presence of TSH in the h7H medium composition as well as the 4-day limited time period of the hormone addition.

3.5.3 LC-MS/MS media analysis for organoid TH production

The organoid production of TH in the media, under a TSH stimulus, was evaluated by assessing their concentration using a previously validated LC-MS/MS analytical method, specifically adapted for our aim. Since the method was initially optimized for plasma and urine matrix, the recovery rates (%) of analytes and the matrix effect in the media analyzed samples were calculated. All analytes displayed a recovery rate ranging from 60% to 90%, while matrix effect was in the range of 64- 99% therefore confirming the validity of the analytical method for these types of matrix as well. The production of TH by organoids is depicted in Figure 4.C as ratio between the concentration of TH in the media recovered from the organoid wells after 4 days of treatment with an additional TSH external stimulus and TH in the blank media, without additional TSH stimulus. TSH stimulation did not significantly trigger changes in either T3 or T4 concentration (1.149 ± 0.149 and 1.109 ± 0.109 for T3 and T4 respectively, P=NS). This could be due to the endogenous quantities of TH in the blank media, the basal TSH stimulus given from the h7H formulation and the presence of a single organoid in each well in our experimental settings.

3.6 Assessment of 3-MNT treatment of 3D culture

3.6.1 MTT assay to determine cell viability with 3-MNT incubation

To screen the concentrations of IYD competitive inhibitor 3-MNT compatible with cell viability, we performed MTT assay on monolayer primary thyrocytes. Figure 5.A shows that no significant difference of viability was found among the tested concentrations. Therefore, we decided to use three concentrations within the range tested: 0.01 µM, 1 µM, 100 µM. This choice was also supported by the concentrations of 3- MNT previously reported in literature (Olker et al., 2021, 2018).

3.6.2 LC-MS/MS media analysis for organoid 3-MNT inhibition of IYD function

To evaluate the interfering action of the inhibitor 3-MNT on the deiodination activity of DEHAL1, we assessed changes in concentrations of MIT and DIT within the culture medium of the organoids upon increasing doses of 3-MNT. Even in these cases, to account for endogenous amounts of TH and precursors in the media and to minimize biological variability effects, we expressed differences between groups as ratios between the treated groups (NaOH + 0.01 - 1 -100 µM 3-MNT) and control vehicle condition (NaOH). As shown in Figure 5.B, adding the inhibitor to the organoid culture medium resulted in an increasing presence of MIT and DIT in the media, correlated with inhibitor concentration. There was a significant difference between the control group and the 100 µM treatment ($p < 0.0001$ for MIT and $p < 0.05$ for DIT), confirming that 3-MNT inhibits IYD's recycling of iodine from TH precursors. However, T3 and T4 levels remained unaffected by 3-MNT. This analysis demonstrates that 3-MNT can inhibit the enzyme IYD, preliminarily candidating our model as feasible for studying the interference of IYD caused by some types of EDs.

3.6.3 Thyroglobulin production analysis by ELISA assay after 3-MNT treatment

Based on evidence from our LC-MS/MS analysis results, organoids were treated with 100 µM 3-MNT for 4 days to shed light on the effect of IYD competitive inhibitor on TH biosynthesis. The resulting data, depicted in Figure 5.C, indicate that the 3-MNT infusion caused a significant 1.4 -fold increase in the production of TG, compared to the control condition (460 ± 16 ng/mL vs 321± 33 ng/mL, $^{**}p < 0.01$). This was in line with the LC-MS/MS analysis data, where IYD inhibition by 3-MNT caused a disruption of iodine recycling mechanism, leading to an increase in the substrates of IYD, MIT and DIT (Figure 5.B) and the activation of a feedback loop mechanism leading to an upstream TG increase (Alikhani et al, 2023).

3.6.4 Gene expression analysis for organoid 3-MNT inhibition of IYD function

To investigate the effect of 3-MNT on the transcription of TH biosynthesis genes in 3D cultures, we evaluated the gene expression of *IYD*, *TG*, *TSHR*, *NIS* and *TPO*, by qRT-PCR assay, after 4-day incubation with the above-mentioned treatment as well. As reported in Figure 5.D, the expression of *TSHR* (fold-change: 0.10, $^{***}p < 0.001$), *NIS* (fold-change: 0.50; $^{*}p < 0.05$) and *TPO* (fold-change: 0.40; $^{***}p < 0.001$) was significantly lower if compared to the control, whereas *IYD* (fold-change: 3.12; $^{**}p < 0.01$) and *TG* (fold-change: 2.31 ;$^{*}p < 0.05$) transcription levels were significantly higher than control condition (vehicle). These results are in line with the LC-MS/MS and ELISA analysis described in the previous paragraphs: the increased expression of *IYD* and *TG* could be considered a counteraction to its inhibition by 3-MNT (Sun et al., 2015). Eventually, the reduction of *THRS*, *NIS* and *TPO* transcripts might be related to the disruption of iodine recycling apparatus system.

4. Discussion

In this study, organoids derived from human non-tumorous primary thyrocytes were collected 8 to 12 days after cell seeding, with each well hosting a single 200 µm organoid. Both 2D and 3D cultures were examined, revealing that 2D cultures expressed thyroid markers but lost phenotype over time, while 3D cultures maintained positiveness for the same markers and preserved thyroid differentiation and functionality, as shown by higher gene expression levels. TEM microscopy showed well-developed structures within organoids, with cells exhibiting active metabolism and mimicking *in vivo* thyroid architecture. Gene expression analysis indicated that 3D cultures better preserved the thyrocyte phenotype. Additionally, 3D cultures produced more thyroglobulin, indicating preserved thyroid function. Treatment with 3-MNT increased MIT and DIT levels, confirming disrupted iodine recycling, while T3 and T4 levels remained unchanged. Further analysis showed that 3-MNT treatment altered TH synthesis gene expression, suggesting a compensatory response to IYD inhibition. Therefore, this 3D system could be considered a tool to investigate thyroid metabolism, disorders and physiology, as an alternative to traditional and already available *in vitro* models.

Recent studies have demonstrated how different aspects and applications of organoid models have been explored. Organoid-based model systems of thyroid have been developed to study autoimmune disease and Graves' hyperthyroidism (van der Vaart et al., 2021), or to produce a thyroid model from human embryonic stem cell to transplant into mice and rescue

hypothyroidism (Romitti et al., 2022). Consequently, thyroid organoids can serve either as thyroid diseases' models or as potential healthy tissues for transplantation in regenerative therapies (Liang et al., 2022; Zhang et al., 2023; Zhao et al., 2022), thus, exploring new approaches beyond animal studies.

In this context, thyroid organoids derived from either tumorous or non-tumorous thyroid cell lines are becoming the gold standard for 3D culture systems. However, 3D thyroid organoids, especially those derived from primary thyrocytes, can display heterogeneity and complexity in cellular composition and in morphogenesis; furthermore, they lack vascularization, which over time leads to a progressive necrotic degeneration, rising from the inner layers of epithelial cells (Zhao et al., 2022). Therefore, improving the currently available protocols and techniques to obtain reproducible 3D thyroid culture systems is considered a crucial issue for the study of thyroid physiology and cancer. Deisenroth and colleagues developed a thyroid microtissue model to screen chemicals that can cause the production of endocrine disruption in humans (Deisenroth et al., 2020). In the development of a 3D model, they observed that primary thyrocytes could self-assemble into organoids with follicle-like structures and produce TH precursors, thyroglobulin, as well as actual TH, T3 and T4. Starting from the achievements of Deisenroth and colleagues' work, we proceeded to develop a novel human 3D thyroid *in vitro* model from primary thyrocytes isolated from healthy donors. Morphological and functional characterization revealed that the 3D cultures preserved a structural and transcriptional memory of the organ physiology, if compared to the corresponding 2D systems. Confocal acquisitions demonstrated that in 2D models the polarized morphology, which is typical of thyroid follicular cells, was lost, despite the unaltered positivity for thyroid markers. On the other hand, 3D models displayed not only positivity for thyroid markers, specifically IYD, TTF-1 and TSHR, as it was provided by the confocal images, but also preservation of thyroid follicular morphology, shown by TEM acquisition. In addition, by confocal as well as brightfield microscopy, it was possible to highlight morphological uniformity in size (about 200 µm diameter) among organoids formed in separate wells of the same 96-well microplates. However, due to technical limitations, fluorescence microscopy did not allow us to explore the inner organization of thyrocytes within the 3D culture. For these reasons, turning to TEM was an inevitable step to reveal the presence of an inner cavity filled with a colloid-like material, surrounded by cuboidal follicular cells, that show a morphological polarity, with microvilli at the apical membrane. In particular, the presence of cell apical microvilli into follicular lumen is related to reabsorption of colloid by phagocytosis (Fujita, 1975). At ultrastructural level, apical microvilli are frequently seen in functional active follicular epithelial cells (Fujita, 1975). Moreover, electron microscopy results show profiles of well-developed RER and Golgi apparatus, which are correlated to cellular activity. In particular, small vesicles arising from Golgi apparatus are typical of protein-secreting cells. Remarkably, ultrastructural analysis demonstrates the presence of a cilium within organoid cells, which witnesses the model reliability. In fact, cilium is a key organelle in the adult thyroid gland of different mammals (human, pig, guinea pig and rabbit) (Wheatley, 2018, 2010, 2005). It is hypothesized that PC possess a sensory activity, linked to intracellular downstream signaling pathways, and it plays a role in the synthesis of TH (Fernández-Santos et al., 2019). All these ultrastructural characteristics observed within cell organoids are highly reminiscent of morphological feature described within thyroid gland; as matter of the fact, they are comparable to those obtained from normal human thyroid as reported by Shiloh et al., 1987 (Shiloh et al., 1987), where fresh surgical human tissue is analyzed. Moreover, thyrocytes from our experimental conditions

exhibited primary cilium as observed in human primary thyrocytes (Fernández-Santos et al., 2019; Utrilla et al., 2015), and ultrastructural features very similar to organoids reported by van der Vaart et al., 2021 (van der Vaart et al., 2021).

Besides the maintenance of morphological features, 3D models proved to be able to express functional thyroid markers as revealed also by protein expression of IYD after 8- 12 days of incubation, while IYD was lost in 2D cultures after the second passage. Furthermore, organoids were transcriptionally more active than the primary P0 and P1 thyrocyte cultures, as the thyroid markers analysed, *IYD*, *TG*, *TSHR*, *TPO*, *NIS*, were significantly higher in 3D conditions, suggesting that recapitulating and preserving the original spatial organization of the primary cells might impact different components of thyroid hormone metabolic machinery. Moreover, even though not significantly, a further supplementation of TSH in the h7H culture medium led to an increase in the transcript levels of the same thyroid markers, after 4 days of incubation with the pituitary hormone, in comparison to the TSH starvation condition. This trend may also be supported by change in TG production that shows an increase, yet not significantly, after 4-day TSH incubation. This non-significance could be due to the organoid formation protocol or to the strong dilution of metabolites released by organoid into the culture medium, because of reduced size of the single organoid in each well compared to the volume of the medium, and lastly to the presence of exogenous TG and THs in commercial sera which might hide small differences in concentrations of released metabolites.

In fact, unlike Deisenroth (Deisenroth et al., 2020), our workflow brought to the formation of a single organoid per well, starting with a smaller number of thyrocyte cells, and did not include the use of any Matrigel matrix at the base of the well except for the little percentage, added to the media, used to guarantee the stability of the 3D conformation. TG production in the two *in vitro* model assays proved to be significantly greater in the 3D culture systems than in the 2D ones. This evidence furtherly supports the results of TEM acquisition as well as thyroid marker gene expression. Indeed, qRT-PCR revealed high transcription levels of *TG*, along with the other highly expressed thyroid markers, pointing out how organoids potentially possess a remarkably active metabolism.

Among the possible thyroid study-related applications, our 3D cultures were developed also with the aim of creating a suitable model to investigate thyroid disorders induced by external threats, in particular EDs, exposure to which may account for the increased incidence of neurodevelopmental disorders and the average reduction in intelligence quotient witnessed in recent decades (Colborn, 2004; Özel and Rüegg, 2023). Therefore, the formation of organoids has been mainly focused on the impact of exogenous compounds, which exert competitive inhibition of IYD, causing the disruption of iodide recycling, which instead is lost in the form of MIT/DIT in urine and plasma (González-Guerrero et al., 2023; Shareef et al., 2023), thus simulating an iodine deficiency situation (Jugan et al., 2010). Hence, to pursue this goal, we followed the expression in our experimental models and then the activity of IYD in presence 3-MNT, that is a product of oxidative stress and a well-known IYD competitive inhibitor (Green, 1968; Olker et al., 2021). Furthermore, since IYD belongs to the NADH-dependent oxidoreductase superfamily, it is plausible that its inhibition would lead to an alteration of the cellular redox and metabolic state. To evaluate the interfering action of the competitor 3-MNT on the deiodination activity of IYD, we first assessed changes in the concentrations of MIT and DIT in organoids' medium upon increasing doses of 3-MNT. Under physiological conditions,

the release of MIT and DIT is usually limited since these two metabolites, substrates of IYD, are catabolized by the thyrocytes to recover the iodine necessary to produce subsequent molecules of T3 and T4 (Czarnocka, 2013). However, when the action of IYD is inhibited or hindered by the presence of interfering molecules, like 3-MNT, which competes with the substrates of the enzyme, the release of MIT and DIT should significantly increase (González-Guerrero et al., 2023). As matter of the fact, in our 3D culture at the highest concentration tested, 3-MNT significantly increased MIT and DIT levels in the media, confirming the role of 3-MNT in inhibiting the recycling of iodine from TH precursor by IYD. These results candidate our organoid model to be a convenient tool for investigating the interfering effects of some xenobiotic molecules (at least members of the same class) on the thyroid system and into the recycling system of iodine. Since 100 μM 3-MNT was the unique effective treatment, further investigations were performed only with the administration of this concentration. qRT-PCR analysis showed that incubation with 3-MNT led to a significant increase in *IYD* and *TG* expression levels, whilst *TSHR*, *NIS* and *TPO* were significantly decreased. Both *IYD* and *TG* enhanced expressions could be explained as a compensatory mechanism in reaction to the enzyme inhibition, thus, reduction of iodine recycling process as already described by Sun et al. 2015 (Alikhani et al, 2023; Sun et al., 2015). TG production was significantly upregulated by 4- day incubation with 100 μM 3-MNT. This result could be seen as a compensatory mechanism as well, following the dysfunction in the iodine recycling mechanism.

Our 3D model presents some limitations. First, primary thyrocytes from human samples are short-lived, usually little available and can reflect the wide variability of patients (Toda et al., 2011). Primary thyrocytes pose challenges in maintaining consistent cultures over extended periods. Then, the variability among samples can potentially affect the reproducibility of experimental outcomes. For this reason, immortalized thyroid-derived cell lines, that maintain responsiveness to TSH and are still actively producing TG, could be seen as a successful step to improve this experimental model (Hopperstad et al., 2021). This approach may enhance model stability and reproducibility, offering a more standardized system for metabolic studies and assessments of endocrine disruptors. Additionally, exploring time- and dose-dependent response of endocrine disruptors beyond 3-MNT would deepen our understanding of this model utility and its potential applications in toxicology and drug development. For instance, a longer exposition may be performed to assess whether lower concentrations of 3-MNT may impact on IYD activity. However, we must consider the lifespan of our organoids: we performed all our assessments on 8–12-day organoids which, as verified by our measurements, preserve their morphology and markers' expression. All these evaluations should be repeated in organoids cultured for a longer age.

Conclusions

In this study we characterized and developed an organoid model of human thyroid that morphologically and functionally conserves the identity of the gland; thus, it could represent an alternative system to investigate thyroid metabolism and physiology, reducing, ultimately, the application of animal models. Finally, due to its sensitivity to 3-MNT treatment leading to IYD inhibition, an event that can also be caused by some EDs, this organoid model could be considered a suitable tool to mimic and analyse the effects EDs on thyroid metabolism.

Acknowledgements

The authors thank Dr. Corinne Dupuy, from Genome Integrity and Cancers, UMR 8200/9019 CNRS, Paris-Saclay University, Gustave Roussy, Villejuif, France for providing stably transfected DEHAL1 HEK293 cell line. The Centre for Instrumentation Sharing of University of Pisa (CISUP) is kindly acknowledged for providing the Sciex QTrap 6500+ mass spectrometer used for the mass spectrometric assays.

Data availability statement

The original contributions presented in the study are included in the article. Further inquiries can be directed to the corresponding authors.

Conflicts of interest

The authors have no relevant financial or non-financial interests to disclose.

Authors contributions

Sofia Cristiani (SC), Andrea Bertolini (AB), Vittoria Carnicelli (VC), Lucia Contu (LC), Valentina Vitelli (VV), Sandra Ghelardoni (SG), Grazia Chiellini (GC), Paola Lenzi (PL), Maria Anita Giambelluca (MAG), Leonardo Rossi (LR), Grazia Rutigliano (GR): Conceptualization, Methodology, Project administration, Validation, Data curation, Visualization, Writing-original draft, Writing-review and editing. Alessandro Saba (AS), Federica Saponaro (FS), Antonietta Raffaella Maria Sabbatini (ARMS), Francesco Fornai (FF), Gabriele Materazzi (GM), Carlo Enrico Ambrosini (CEA), Ranieri Bizzarri (RB), Riccardo Zucchi (RZ): review and editing.

Funding

This work was supported by a grant from University of Pisa to GR, RB, SG, GC, ARMS, PL, FS, VC (PRA PRA_2020_77).

References

Alikhani P., González Guerrero C., Bertolini A., Vitelli V., Borsò M., Regojo R. M., Peluso T., Salas-Lucia F., de la Vieja A., Saba A., Zucchi R., M.J.C., 2023. Dehal1 Deficiency disrupts Thyroglobulin homeostasis and Impairs Iodine Storage. 45th Annu. Meet. Eur. Thyroid Assoc.

Ameziane-El-Hassani, R., Morand, S., Boucher, J.-L., Frapart, Y.-M., Apostolou, D., Agnandji, D., Gnidehou, S., Ohayon, R., Noël-Hudson, M.-S., Francon, J., Lalaoui, K., Virion, A., Dupuy, C., 2005. Dual oxidase-2 has an intrinsic Ca2+-dependent H2O2-generating activity. J. Biol. Chem. 280, 30046–30054. https://doi.org/10.1074/jbc.M500516200

Antonica, F., Kasprzyk, D.F., Opitz, R., Iacovino, M., Liao, X.-H., Dumitrescu, A.M., Refetoff, S., Peremans, K., Manto, M., Kyba, M., Costagliola, S., 2012. Generation of functional thyroid from embryonic stem cells. Nature 491, 66–71. https://doi.org/10.1038/nature11525

Arvan, P., Kim, P.S., Kuliawat, R., Prabakaran, D., Muresan, Z., Yoo, S.E.U.N., Hossain, S.A.B.U., 1997. Intracellular Protein Transport to the Thyrocyte Plasma Membrane: Potential Implications for Thyroid Physiology. Thyroid® 7, 89–105. https://doi.org/10.1089/thy.1997.7.89

Asawasinsopon, R., Prapamontol, T., Prakobvitayakit, O., Vaneesorn, Y., Mangklabruks, A., Hock, B., 2006. The association between organochlorine and thyroid hormone levels in cord serum: a study from northern Thailand. Environ. Int. 32, 554–559. https://doi.org/10.1016/j.envint.2006.01.001

Bandini, L., Sacripanti, G., Borsò, M., Tartaria, M., Fogliaro, M.P., Giannini, G., Carnicelli, V., Figuccia, M.E., Verlotta, S., De Antoni, F., Zucchi, R., Ghelardoni, S., 2022. Exogenous 3-Iodothyronamine (T(1)AM) Can Affect Phosphorylation of Proteins Involved on Signal Transduction Pathways in In Vitro Models of Brain Cell Lines, but These Effects Are Not Strengthened by Its Catabolite, 3-Iodothyroacetic Acid (TA(1)). Life (Basel, Switzerland) 12. https://doi.org/10.3390/life12091352

Belforte, F.S., Targovnik, A.M., González-Lebrero, R.M., Osorio Larroche, C., Citterio, C.E., González-Sarmiento, R., Miranda, M. V, Targovnik, H.M., Rivolta, C.M., 2015. Kinetic characterization of human thyroperoxidase. Normal and pathological enzyme expression in Baculovirus system: a molecular model of functional expression. Mol. Cell. Endocrinol. 404, 9–15. https://doi.org/10.1016/j.mce.2014.12.026

Bianco, A.C., Kim, B.W., 2006. Deiodinases: implications of the local control of thyroid hormone action. J. Clin. Invest. 116, 2571–2579. https://doi.org/10.1172/JCI29812

Borsò, M., Agretti, P., Zucchi, R., Saba, A., 2022. Mass spectrometry in the diagnosis of thyroid disease and in the study of thyroid hormone metabolism. Mass Spectrom. Rev. 41, 443–468. https://doi.org/10.1002/mas.21673

Bravo, S.B., Garcia-Rendueles, M.E.R., Garcia-Rendueles, A.R., Rodrigues, J.S., Perez-Romero, S., Garcia-Lavandeira, M., Suarez-Fariña, M., Barreiro, F., Czarnocka, B., Senra, A., Lareu, M. V, Rodriguez-Garcia, J., Cameselle-Teijeiro, J., Alvarez, C. V, 2013. Humanized medium (h7H) allows long-term primary follicular thyroid cultures from human normal thyroid, benign neoplasm, and cancer. J. Clin. Endocrinol. Metab. 98, 2431–2441. https://doi.org/10.1210/jc.2012-3812

Carvalho, D.P., Dupuy, C., 2013. Role of the NADPH Oxidases DUOX and NOX4 in Thyroid Oxidative Stress. Eur. Thyroid J. 2, 160–167. https://doi.org/10.1159/000354745

Chevrier, J., Eskenazi, B., Holland, N., Bradman, A., Barr, D.B., 2008. Effects of exposure to polychlorinated biphenyls and organochlorine pesticides on thyroid function during pregnancy. Am. J. Epidemiol. 168, 298–310. https://doi.org/10.1093/aje/kwn136

Citterio, C.E., Targovnik, H.M., Arvan, P., 2019. The role of thyroglobulin in thyroid hormonogenesis. Nat. Rev. Endocrinol. 15, 323–338. https://doi.org/10.1038/s41574-019-0184-8

Colborn, T., 2004. Neurodevelopment and endocrine disruption. Environ. Health Perspect.

663 112, 944–949. https://doi.org/10.1289/ehp.6601

664 Czarnocka, B., 2013. The proteins of iodine metabolism in the pathophysiology of the thyroid
665 gland. Thyroid Res. https://doi.org/10.1186/1756-6614-6-S2-A13

666 Dalir Abdolahinia, E., Han, X., 2023. The Three-Dimensional In Vitro Cell Culture Models
667 in the Study of Oral Cancer Immune Microenvironment. Cancers (Basel). 15.
668 https://doi.org/10.3390/cancers15174266

669 de Escobar, G.M., Obregón, M.J., del Rey, F.E., 2007. Iodine deficiency and brain
670 development in the first half of pregnancy. Public Health Nutr. 10, 1554–1570.
671 https://doi.org/10.1017/S1368980007360928

672 Deisenroth, C., Soldatow, V.Y., Ford, J., Stewart, W., Brinkman, C., LeCluyse, E.L.,
673 MacMillan, D.K., Thomas, R.S., 2020. Development of an In Vitro Human Thyroid
674 Microtissue Model for Chemical Screening. Toxicol. Sci. 174, 63–78.
675 https://doi.org/10.1093/toxsci/kfz238

676 Edmondson, R., Broglie, J.J., Adcock, A.F., Yang, L., 2014. Three-dimensional cell culture
677 systems and their applications in drug discovery and cell-based biosensors. Assay Drug
678 Dev. Technol. 12, 207–218. https://doi.org/10.1089/adt.2014.573

679 Estrada, J.M., Soldin, D., Buckey, T.M., Burman, K.D., Soldin, O.P., 2014. Thyrotropin
680 isoforms: implications for thyrotropin analysis and clinical practice. Thyroid 24, 411–
681 423. https://doi.org/10.1089/thy.2013.0119

682 Fabbro, D., Di Loreto, C., Beltrami, C.A., Belfiore, A., Di Lauro, R., Damante, G., 1994.
683 Expression of thyroid-specific transcription factors TTF-1 and PAX-8 in human thyroid
684 neoplasms. Cancer Res. 54, 4744–4749.

685 Fekete, C., Lechan, R.M., 2014. Central regulation of hypothalamic-pituitary-thyroid axis
686 under physiological and pathophysiological conditions. Endocr. Rev. 35, 159–194.
687 https://doi.org/10.1210/er.2013-1087

688 Fernández-Santos, J.M., Utrilla, J.C., Vázquez-Román, V., Villar-Rodríguez, J.L., Gutiérrez-
689 Avilés, L., Martín-Lacave, I., 2019. Primary Cilium in the Human Thyrocyte: Changes
690 in Frequency and Length in Relation to the Functional Pathology of the Thyroid Gland.
691 Thyroid 29, 595–606. https://doi.org/10.1089/thy.2018.0401

692 Fujita, H., 1975. Fine structure of the thyroid gland. Int. Rev. Cytol. 40, 197–280.
693 https://doi.org/10.1016/s0074-7696(08)60954-7

694 Gereben, B., McAninch, E.A., Ribeiro, M.O., Bianco, A.C., 2015. Scope and limitations of
695 iodothyronine deiodinases in hypothyroidism. Nat. Rev. Endocrinol. 11, 642–652.
696 https://doi.org/10.1038/nrendo.2015.155

697 Gillam, M.P., Sidhaye, A.R., Lee, E.J., Rutishauser, J., Stephan, C.W., Kopp, P., 2004.
698 Functional characterization of pendrin in a polarized cell system. Evidence for pendrin-
699 mediated apical iodide efflux. J. Biol. Chem. 279, 13004–13010.
700 https://doi.org/10.1074/jbc.M313648200

701 Gnidehou, S., Caillou, B., Talbot, M., Ohayon, R., Kaniewski, J., Noël-Hudson, M.-S.,
702 Morand, S., Agnangji, D., Sezan, A., Courtin, F., Virion, A., Dupuy, C., 2004.
703 Iodotyrosine dehalogenase 1 (DEHAL1) is a transmembrane protein involved in the
704 recycling of iodide close to the thyroglobulin iodination site. FASEB J. Off. Publ. Fed.
705 Am. Soc. Exp. Biol. 18, 1574–1576. https://doi.org/10.1096/fj.04-2023fje

706 Godlewska, M., Góra, M., Buckle, A.M., Porebski, B.T., Kemp, E.H., Sutton, B.J.,
707 Czarnocka, B., Banga, J.P., 2014. A redundant role of human thyroid peroxidase
708 propeptide for cellular, enzymatic, and immunological activity. Thyroid 24, 371–382.
709 https://doi.org/10.1089/thy.2013.0127

710 González-Guerrero, C., Borsò, M., Alikhani, P., Alcaina, Y., Salas-Lucia, F., Liao, X.-H.,
711 García-Giménez, J., Bertolini, A., Martin, D., Moratilla, A., Mora, R., Buño-Soto, A.,
712 Mani, A.R., Bernal, J., Saba, A., de Miguel, M.P., Refetoff, S., Zucchi, R., Moreno, J.C.,
713 2023. Iodotyrosines Are Biomarkers for Preclinical Stages of Iodine-Deficient
714 Hypothyroidism in Dehal1-Knockout Mice. Thyroid 33, 752–761.
715 https://doi.org/10.1089/thy.2022.0537

716 Green, W.L., 1968. Inhibition of thyroidal iodotyrosine deiodination by tyrosine analogues.
717 Endocrinology 83, 336–347. https://doi.org/10.1210/endo-83-2-336

718 Haddow, J.E., Palomaki, G.E., Allan, W.C., Williams, J.R., Knight, G.J., Gagnon, J., O'Heir,
719 C.E., Mitchell, M.L., Hermos, R.J., Waisbren, S.E., Faix, J.D., Klein, R.Z., 1999.
720 Maternal thyroid deficiency during pregnancy and subsequent neuropsychological
721 development of the child. N. Engl. J. Med. 341, 549–555.
722 https://doi.org/10.1056/NEJM199908193410801

723 Hetzel, B.S., 2000. Iodine and neuropsychological development. J. Nutr. 130, 493S-495S.
724 https://doi.org/10.1093/jn/130.2.493S

725 Hopperstad, K., Truschel, T., Wahlicht, T., Stewart, W., Eicher, A., May, T., Deisenroth, C.,
726 2021. Characterization of Novel Human Immortalized Thyroid Follicular Epithelial Cell
727 Lines. Appl. Vitr. Toxicol. 7, 39–49. https://doi.org/10.1089/aivt.2020.0027

728 Hwang, D.G., Choi, Y.-M., Jang, J., 2021. 3D Bioprinting-Based Vascularized Tissue
729 Models Mimicking Tissue-Specific Architecture and Pathophysiology for in vitro
730 Studies. Front. Bioeng. Biotechnol. 9, 685507.
731 https://doi.org/10.3389/fbioe.2021.685507

732 Jubelin, C., Muñoz-Garcia, J., Griscom, L., Cochonneau, D., Ollivier, E., Heymann, M.-F.,
733 Vallette, F.M., Oliver, L., Heymann, D., 2022. Three-dimensional in vitro culture
734 models in oncology research. Cell Biosci. 12, 155. https://doi.org/10.1186/s13578-022-
735 00887-3

736 Jugan, M.-L., Levi, Y., Blondeau, J.-P., 2010. Endocrine disruptors and thyroid hormone
737 physiology. Biochem. Pharmacol. 79, 939–947.
738 https://doi.org/10.1016/j.bcp.2009.11.006

739 Kogai, T., Endo, T., Saito, T., Miyazaki, A., Kawaguchi, A., Onaya, T., 1997. Regulation by
740 thyroid-stimulating hormone of sodium/iodide symporter gene expression and protein
741 levels in FRTL-5 cells. Endocrinology 138, 2227–2232.
742 https://doi.org/10.1210/endo.138.6.5189

743 Kurmann, A.A., Serra, M., Hawkins, F., Rankin, S.A., Mori, M., Astapova, I., Ullas, S., Lin,
744 S., Bilodeau, M., Rossant, J., Jean, J.C., Ikonomou, L., Deterding, R.R., Shannon, J.M.,
745 Zorn, A.M., Hollenberg, A.N., Kotton, D.N., 2015. Regeneration of Thyroid Function
746 by Transplantation of Differentiated Pluripotent Stem Cells. Cell Stem Cell 17, 527–
747 542. https://doi.org/10.1016/j.stem.2015.09.004

748 Lelièvre, S.A., Kwok, T., Chittiboyina, S., 2017. Architecture in 3D cell culture: An essential
749 feature for in vitro toxicology. Toxicol. Vitr. an Int. J. Publ. Assoc. with BIBRA 45,

287–295. https://doi.org/10.1016/j.tiv.2017.03.012

Liang, J., Li, X., Dong, Y., Zhao, B., 2022. Modeling Human Organ Development and Diseases With Fetal Tissue-Derived Organoids. Cell Transplant. 31, 9636897221124480. https://doi.org/10.1177/09636897221124481

Livak, K.J., Schmittgen, T.D., 2001. Analysis of relative gene expression data using real-time quantitative PCR and the 2(-Delta Delta C(T)) Method. Methods 25, 402–408. https://doi.org/10.1006/meth.2001.1262

Longmire, T.A., Ikonomou, L., Hawkins, F., Christodoulou, C., Cao, Y., Jean, J.C., Kwok, L.W., Mou, H., Rajagopal, J., Shen, S.S., Dowton, A.A., Serra, M., Weiss, D.J., Green, M.D., Snoeck, H.-W., Ramirez, M.I., Kotton, D.N., 2012. Efficient derivation of purified lung and thyroid progenitors from embryonic stem cells. Cell Stem Cell 10, 398–411. https://doi.org/10.1016/j.stem.2012.01.019

Lopez-Espinosa, M.-J., Vizcaino, E., Murcia, M., Llop, S., Espada, M., Seco, V., Marco, A., Rebagliato, M., Grimalt, J.O., Ballester, F., 2009. Association between thyroid hormone levels and 4,4'-DDE concentrations in pregnant women (Valencia, Spain). Environ. Res. 109, 479–485. https://doi.org/10.1016/j.envres.2009.02.003

Luongo, C., Dentice, M., Salvatore, D., 2019. Deiodinases and their intricate role in thyroid hormone homeostasis. Nat. Rev. Endocrinol. 15, 479–488. https://doi.org/10.1038/s41574-019-0218-2

Matuszewski, B.K., Constanzer, M.L., Chavez-Eng, C.M., 2003. Strategies for the assessment of matrix effect in quantitative bioanalytical methods based on HPLC-MS/MS. Anal. Chem. 75, 3019–3030. https://doi.org/10.1021/ac020361s

Ohno, M., Zannini, M., Levy, O., Carrasco, N., di Lauro, R., 1999. The paired-domain transcription factor Pax8 binds to the upstream enhancer of the rat sodium/iodide symporter gene and participates in both thyroid-specific and cyclic-AMP-dependent transcription. Mol. Cell. Biol. 19, 2051–2060. https://doi.org/10.1128/MCB.19.3.2051

Olker, J.H., Haselman, J.T., Kosian, P.A., Donnay, K.G., Korte, J.J., Blanksma, C., Hornung, M.W., Degitz, S.J., 2018. Evaluating Iodide Recycling Inhibition as a Novel Molecular Initiating Event for Thyroid Axis Disruption in Amphibians. Toxicol. Sci. 166, 318–331. https://doi.org/10.1093/toxsci/kfy203

Olker, J.H., Korte, J.J., Denny, J.S., Haselman, J.T., Hartig, P.C., Cardon, M.C., Hornung, M.W., Degitz, S.J., 2021. In vitro screening for chemical inhibition of the iodide recycling enzyme, iodotyrosine deiodinase. Toxicol. Vitr. an Int. J. Publ. Assoc. with BIBRA 71, 105073. https://doi.org/10.1016/j.tiv.2020.105073

Özel, F., Rüegg, J., 2023. Exposure to endocrine-disrupting chemicals and implications for neurodevelopment. Dev. Med. Child Neurol. 65, 1005–1011. https://doi.org/10.1111/dmcn.15551

Portulano, C., Paroder-Belenitsky, M., Carrasco, N., 2014. The Na+/I- symporter (NIS): mechanism and medical impact. Endocr. Rev. 35, 106–149. https://doi.org/10.1210/er.2012-1036

Román, G.C., Ghassabian, A., Bongers-Schokking, J.J., Jaddoe, V.W. V, Hofman, A., de Rijke, Y.B., Verhulst, F.C., Tiemeier, H., 2013. Association of gestational maternal hypothyroxinemia and increased autism risk. Ann. Neurol. 74, 733–742.

https://doi.org/10.1002/ana.23976

Romitti, M., Tourneur, A., de Faria da Fonseca, B., Doumont, G., Gillotay, P., Liao, X.-H., Eski, S.E., Van Simaeys, G., Chomette, L., Lasolle, H., Monestier, O., Kasprzyk, D.F., Detours, V., Singh, S.P., Goldman, S., Refetoff, S., Costagliola, S., 2022. Transplantable human thyroid organoids generated from embryonic stem cells to rescue hypothyroidism. Nat. Commun. 13, 7057. https://doi.org/10.1038/s41467-022-34776-7

Samimi, H., Atlasi, R., Parichehreh-Dizaji, S., Khazaei, S., Akhavan Rahnama, M., Seifirad, S., Haghpanah, V., 2021. A systematic review on thyroid organoid models: time-trend and its achievements. Am. J. Physiol. Endocrinol. Metab. 320, E581–E590. https://doi.org/10.1152/ajpendo.00479.2020

Sewell, W., Lin, R.-Y., 2014. Generation of thyroid follicular cells from pluripotent stem cells: potential for regenerative medicine. Front. Endocrinol. (Lausanne). 5, 96. https://doi.org/10.3389/fendo.2014.00096

Shankaran, A., Prasad, K., Chaudhari, S., Brand, A., Satyamoorthy, K., 2021. Advances in development and application of human organoids. 3 Biotech 11, 257. https://doi.org/10.1007/s13205-021-02815-7

Shareef, R., Furman, A., Watanabe, Y., Bruellman, R., Abdullah, M.A., Dumitresu, A.M., Refetoff, S., Bertolini, A., Borsò, M., Saba, A., Zucchi, R., Weiss, R.E., 2023. Congenital Hypothyroidism in Two Sudanese Families Harboring a Novel Iodotyrosine Deiodinase Mutation (IYD R279C). Thyroid 33, 261–266. https://doi.org/10.1089/thy.2022.0492

Shiloh, H., Iancu, T.C., Sheinfeld, M., Kraiem, Z., 1987. The influence of cryopreservation on the ultrastructural morphology of human thyroid cells. Cryobiology 24, 303–310. https://doi.org/10.1016/0011-2240(87)90034-4

Sun, X., Zhang, X., Jiang, Y., Bao, S., Shan, Z., Teng, W., 2015. Expression of Iodotyrosine Deiodinase in Thyroid and Other Organs in Iodine-Deficient and Iodine-Excess Rats. Biol. Trace Elem. Res. 167, 272–279. https://doi.org/10.1007/s12011-015-0328-1

Tannenbaum, J., Bennett, B.T., 2015. Russell and Burch's 3Rs then and now: the need for clarity in definition and purpose. J. Am. Assoc. Lab. Anim. Sci. 54, 120–132.

Toda, S., Aoki, S., Uchihashi, K., Matsunobu, A., Yamamoto, M., Ootani, A., Yamasaki, F., Koike, E., Sugihara, H., 2011. Culture Models for Studying Thyroid Biology and Disorders. ISRN Endocrinol. 2011, 275782. https://doi.org/10.5402/2011/275782

Utrilla, J.C., Gordillo-Martínez, F., Gómez-Pascual, A., Fernández-Santos, J.M., Garnacho, C., Vázquez-Román, V., Morillo-Bernal, J., García-Marín, R., Jiménez-García, A., Martín-Lacave, I., 2015. Comparative study of the primary cilia in thyrocytes of adult mammals. J. Anat. 227, 550–560. https://doi.org/10.1111/joa.12360

van der Vaart, J., Bosmans, L., Sijbesma, S.F., Knoops, K., van de Wetering, W.J., Otten, H.G., Begthel, H., Borel Rinkes, I.H.M., Korving, J., Lentjes, E.G.W.M., Lopez-Iglesias, C., Peters, P.J., van Santen, H.M., Vriens, M.R., Clevers, H., 2021. Adult mouse and human organoids derived from thyroid follicular cells and modeling of Graves' hyperthyroidism. Proc. Natl. Acad. Sci. U. S. A. 118. https://doi.org/10.1073/pnas.2117017118

Wang, Y., Li, W., Phay, J.E., Shen, R., Pellegata, N.S., Saji, M., Ringel, M.D., de la

Chapelle, A., He, H., 2016. Primary Cell Culture Systems for Human Thyroid Studies. Thyroid 26, 1131–1140. https://doi.org/10.1089/thy.2015.0518

Wheatley, D.N., 2018. The primary cilium - once a "rudimentary" organelle that is now a ubiquitous sensory cellular structure involved in many pathological disorders. J. Cell Commun. Signal. 12, 211–216. https://doi.org/10.1007/s12079-017-0436-0

Wheatley, D.N., 2010. Another decade of advances in research on primary cilia, porosomes and neosis: some passing thoughts at 70. Cell Biol. Int. https://doi.org/10.1042/CBI20100119

Wheatley, D.N., 2005. Landmarks in the first hundred years of primary (9+0) cilium research. Cell Biol. Int. 29, 333–339. https://doi.org/10.1016/j.cellbi.2005.03.001

Wright, E.M., Turk, E., 2004. The sodium/glucose cotransport family SLC5. Pflugers Arch. 447, 510–518. https://doi.org/10.1007/s00424-003-1063-6

Yokoyama, N., Taurog, A., 1988. Porcine thyroid peroxidase: relationship between the native enzyme and an active, highly purified tryptic fragment. Mol. Endocrinol. 2, 838–844. https://doi.org/10.1210/mend-2-9-838

Zhang, Y., Fu, M., Wang, H., Sun, H., 2023. Advances in the Construction and Application of Thyroid Organoids. Physiol. Res. 72, 557–564. https://doi.org/10.33549/physiolres.935102

Zhao, Z., Chen, X., Dowbaj, A.M., Sljukic, A., Bratlie, K., Lin, L., Fong, E.L.S., Balachander, G.M., Chen, Z., Soragni, A., Huch, M., Zeng, Y.A., Wang, Q., Yu, H., 2022. Organoids. Nat. Rev. Methods Prim. 2. https://doi.org/10.1038/s43586-022-00174-y

Zimmermann, M.B., Jooste, P.L., Pandav, C.S., 2008. Iodine-deficiency disorders. Lancet (London, England) 372, 1251–1262. https://doi.org/10.1016/S0140-6736(08)61005-3

Journal Pre-proof

Figure captions

Figure 1. **Thyroid organoid formation and immunofluorescence characterization**. A) Brightfield images depicting digested primary thyrocytes and 2D thyrocytes at confluence (A1-2). Organoid formation: once thyrocytes reached confluence, they were seeded in Nunclon Sphera™ microplates to form organoid that could be seen in the following 24 hours (A3); organoid after 7 days (A4); after 10 days from formation (A5); 3D cultures were then collected for characterization analyses. Scale bar: 100 µm. B) Confocal images of 2D P0 primary thyrocytes expressing TSHR (magenta A3), TTF-1 (red B3), IYD (green A2), and α-Tubulin (cyan B2). Nuclei are stained with DAPI. Scale bar: 25 µm (B); 10 µm (A). C) Confocal images of 3D cultures (A; B; C; D) expressing TSHR (magenta A3), TTF-1 (red B3), IYD (green C2), and Phalloidin (white A2). The same organoids in D1 are also shown in brightfield microscopy in D2. Nuclei are stained with DAPI. Scale bar: 100 µm (A; C); 25 µm (B).

Figure 2. Light microscopy and transmission electron microscopy characterization. A) Representative pictures at light microscopy and transmission electron microscopy (TEM) from a human non-tumorous thyroid organoid. A1, Toluidine blue histochemistry was carried out on semi-thin slices (1 μm-thick) in which an organoid shown the inner cavity (*), well evident at ultrastructural level (A2). In the cell apical surface microvilli protrude within the cavity (A3, arrows). In sub-apical cytoplasm droplets are evident (A4, arrows) Scale bar: A1= 12.5 μm; A2= 0.6 μm; A3= 300 nm; A4= 2.5 □m. B) TEM representative picture of organoid epithelial cell: B1 cell junctions (arrows), B2 dilated cisternae of RER, B3 Golgi apparatus and small vesicles (V), B4 numerous lysosome-like organelles. M=mitochondria, N=nucleus, L=Lysosome-like structure. PC=primary cilium. RER=rough endoplasmic reticulum. Scale bar: B1= 150 nm; B2= 0.23 μm; B3= 300 nm; B4= 300 nm**.**

Figure 3. Expression of thyroid markers in 2D cells and organoids. A) Gene expression: relative expressions of thyroid markers in primary thyrocytes at passages 0 (P0, reference sample), 1 (P1) and organoids (3D) by qRT-PCR. 2D (P0 and P1) and 3D culture sample data were normalized to internal reference control (*GAPDH*) and expressed as the relative expression (fold-change) to P0 thyrocytes. The results are expressed as mean ± S.E.M. Statistical analysis was performed through one-way ANOVA and post hoc test Tukey, with a significant p value *p<0.05, **p<0.01, ***p<0.001; N= 3. B) Western blotting with IYD antibody in 2D cells, organoid lysates and thyroid extract. B1) Lysates of primary thyroid cells at passages 0 (P0), 1 (P1), and 2 (P2) and thyroid extract (C+): in lane P0 and C+, the band between 25 and 37 kDa is specific, being seen in presence of antibody anti IYD but not after incubation with blocking peptide (B2). This band disappears following incubation with blocking peptide, signifying the specificity of IYD. B3) α-actin (42 kDa) in 2D cell lysates and tissues extract (C+). B4) Lysates from cells at passage 0 (P0), from a pool of organoids cultured in Nunclon Sphere™ (3D), from HEK293 cells transfected with IYD (DEHAL1) (C); immunoblotting with anti-IYD highlighted a band between 25 and 37 kDa in all lanes. B5) α-actin (42 kDa) in 2D cell lysate and organoids. Numbers are molecular weight (kDa); M, protein standards (Precision Plus Protein™ Kaleidoscope™ Prestained Protein Standards #1610375 Biorad). C) TG ELISA assay in exhausted media of 2D, at P0 and P1, and 3D cultures. The results are expressed as mean ± S.E.M. Statistical analysis is performed through *t*-test, with a significant p value ****p<0.0001; N= 3.

Figure 4. Effects of TSH stimulation. A) TG concentration in media by ELISA assay on 3D cultures with or without 2 mU/mL TSH incubation for 4 days. The results are expressed as mean ± S.E.M. Statistical analysis was performed through t-test, P=NS; N= 3. B) Relative expressions of thyroid markers in 3D cultures after incubation with 2 mU/mL TSH (TSH), as opposed to no TSH further addition (no TSH), for 4 days, by qRT-PCR. The culture sample data were normalized to internal reference control (*GAPDH*) and expressed as the relative expression (fold-change) to no TSH. The results are expressed as mean ± S.E.M. Statistical analysis was performed by t-test. P=NS; N= 3. C) Organoid TH production in media samples. The production rate of TH by organoids is expressed as ratio between the concentration of TH in the media recovered from the organoids wells after 4 days of treatment with an additional TSH external stimulus and TH in the blank media, without additional TSH stimulus.

Experiments were conducted in triplicate. Results are expressed as Mean ± S.E.M. Statistical analysis was performed by *t*-test. P=NS

Figure 5. Effect of the IYD inhibitor 3-mononitrotyrosine (3-MNT) on thyroid function. A) MTT assay on monolayer primary thyrocytes to test cell viability after 24-hour incubation with increasing concentrations of 3-MNT for 4 days. The results are expressed as mean ± S.E.M. of 4 technical replicates. B) Effect of 3-MNT inhibition on IYD enzyme. Differences between groups are expressed as ratios between the treated groups (0.01-1-100 μM 3-MNT) and the control vehicle condition (NaOH). Experiments were all conducted in triplicate. Results are expressed as Mean ± S.E.M. Two-way ANOVA and Tukey's multiple comparison test were performed to evaluate statistical differences between groups; * $p<0.05$, **** $p<0.001$ vs control § $p<0.001$ vs 0.01/1 μM MNT treatment. C) TG ELISA assay on 3D culture after incubation with 3-MNT 100 μM for 4 days. The results are expressed as mean ± S.E.M. Statistical analysis was performed through *t*-test, with a significant p value **$p<0.01$; N= 3. D) Relative expressions of thyroid markers in 3D cultures after incubation with 100 μM 3-MNT for 4 days, by qRT-PCR. Sample data from treatment condition (100 μM 3-MNT) were normalized to internal reference control (*GAPDH*) and expressed as the relative expression (fold-change) vs control (0.05 mM NaOH). The results are expressed as mean ± S.E.M. Statistical analysis was performed by *t*-test, with a significant p value *$p<0.05$, **$p<0.01$, ***$p<0.001$; N= 3.

Journal Pre-proof

Figure captions

Figure 1. **Thyroid organoid formation and immunofluorescence characterization**. A) Brightfield images depicting digested primary thyrocytes and 2D thyrocytes at confluence (A1-2). Organoid formation: once thyrocytes reached confluence, they were seeded in Nunclon Sphera™ microplates to form organoid that could be seen in the following 24 hours (A3); organoid after 7 days (A4); after 10 days from formation (A5); 3D cultures were then collected for characterization analyses. Scale bar: 100 µm. B) Confocal images of 2D P0 primary thyrocytes expressing TSHR (magenta A3), TTF-1 (red B3), IYD (green A2), and α-Tubulin (cyan B2). Nuclei are stained with DAPI. Scale bar: 25 µm (B); 10 µm (A). C) Confocal images of 3D cultures (A; B; C; D) expressing TSHR (magenta A3), TTF-1 (red B3), IYD (green C2), and Phalloidin (white A2). The same organoids in D1 are also shown in brightfield microscopy in D2. Nuclei are stained with DAPI. Scale bar: 100 µm (A; C); 25 µm (B).

Figure 2. Light microscopy and transmission electron microscopy characterization. A) Representative pictures at light microscopy and transmission electron microscopy (TEM) from a human non-tumorous thyroid organoid. A1, Toluidine blue histochemistry was carried out on semi-thin slices (1 µm-thick) in which an organoid shown the inner cavity (*), well evident at ultrastructural level (A2). In the cell apical surface microvilli protrude within the cavity (A3, arrows). In sub-apical cytoplasm droplets are evident (A4, arrows) Scale bar: A1= 12.5 µm; A2= 0.6 µm; A3= 300 nm; A4= 2.5 □m. B) TEM representative picture of organoid epithelial cell: B1 cell junctions (arrows), B2 dilated cisternae of RER, B3 Golgi apparatus and small vesicles (V), B4 numerous lysosome-like organelles. M=mitochondria, N=nucleus, L=Lysosome-like structure. PC=primary cilium. RER=rough endoplasmic reticulum. Scale bar: B1= 150 nm; B2= 0.23 µm; B3= 300 nm; B4= 300 nm**.**

Figure 3. Expression of thyroid markers in 2D cells and organoids. A) Gene expression: relative expressions of thyroid markers in primary thyrocytes at passages 0 (P0, reference sample), 1 (P1) and organoids (3D) by qRT-PCR. 2D (P0 and P1) and 3D culture sample data were normalized to internal reference control (*GAPDH*) and expressed as the relative expression (fold-change) to P0 thyrocytes. The results are expressed as mean ± S.E.M. Statistical analysis was performed through one-way ANOVA and post hoc test Tukey, with a significant p value *p<0.05, **p<0.01, ***p<0.001; N= 3. B) Western blotting with IYD antibody in 2D cells, organoid lysates and thyroid extract. B1) Lysates of primary thyroid cells at passages 0 (P0), 1 (P1), and 2 (P2) and thyroid extract (C+): in lane P0 and C+, the band between 25 and 37 kDa is specific, being seen in presence of antibody anti IYD but not after incubation with blocking peptide (B2). This band disappears following incubation with blocking peptide, signifying the specificity of IYD. B3) α-actin (42 kDa) in 2D cell lysates and tissues extract (C+). B4) Lysates from cells at passage 0 (P0), from a pool of organoids cultured in Nunclon Sphere™ (3D), from HEK293 cells transfected with IYD (DEHAL1) (C); immunoblotting with anti-IYD highlighted a band between 25 and 37 kDa in all lanes. B5) α-actin (42 kDa) in 2D cell lysate and organoids. Numbers are molecular weight (kDa); M, protein standards (Precision Plus Protein™ Kaleidoscope™ Prestained Protein Standards #1610375 Biorad). C) TG ELISA assay in exhausted media of 2D, at P0 and P1, and 3D cultures. The results are expressed as mean ± S.E.M. Statistical analysis is performed through *t*-test, with a significant p value ****p<0.0001; N= 3.

Figure 4. Effects of TSH stimulation. A) TG concentration in media by ELISA assay on 3D cultures with or without 2 mU/mL TSH incubation for 4 days. The results are expressed as mean ± S.E.M. Statistical analysis was performed through t-test, P=NS; N= 3. B) Relative expressions of thyroid markers in 3D cultures after incubation with 2 mU/mL TSH (TSH), as opposed to no TSH further addition (no TSH), for 4 days, by qRT-PCR. The culture sample data were normalized to internal reference control (*GAPDH*) and expressed as the relative expression (fold-change) to no TSH. The results are expressed as mean ± S.E.M. Statistical analysis was performed by t-test. P=NS; N= 3. C) Organoid TH production in media samples. The production rate of TH by organoids is expressed as ratio between the concentration of TH in the media recovered from the organoids wells after 4 days of treatment with an additional TSH external stimulus and TH in the blank media, without additional TSH stimulus. Experiments were conducted in triplicate. Results are expressed as Mean ± S.E.M. Statistical analysis was performed by *t*-test. P=NS

Figure 5. Effect of the IYD inhibitor 3-mononitrotyrosine (3-MNT) on thyroid function. A) MTT assay on monolayer primary thyrocytes to test cell viability after 24-hour incubation with increasing concentrations of 3-MNT for 4 days. The results are expressed as mean ± S.E.M. of 4 technical replicates. B) Effect of 3-MNT inhibition on IYD enzyme. Differences between groups are expressed as ratios between the treated groups (0.01-1-100 µM 3-MNT) and the control vehicle condition (NaOH). Experiments were all conducted in triplicate. Results are expressed as Mean ± S.E.M. Two-way ANOVA and Tukey's multiple comparison test were performed to evaluate statistical differences between groups; * $p<0.05$, **** $p<0.001$ vs control § $p<0.001$ vs 0.01/1 µM MNT treatment. C) TG ELISA assay on 3D culture after incubation with 3-MNT 100 µM for 4 days. The results are expressed as mean ± S.E.M. Statistical analysis was performed through *t*-test, with a significant p value **$p<0.01$; N= 3. D) Relative expressions of thyroid markers in 3D cultures after incubation with 100 µM 3-MNT for 4 days, by qRT-PCR. Sample data from treatment condition (100 µM 3-MNT) were normalized to internal reference control (*GAPDH*) and expressed as the relative expression (fold-change) vs control (0.05 mM NaOH). The results are expressed as mean ± S.E.M. Statistical analysis was performed by *t*-test, with a significant p value *$p<0.05$, **$p<0.01$, ***$p<0.001$; N= 3.

Journal Pre-proof

Journal Pre-proof

Journal Pre-proof

Figure 1

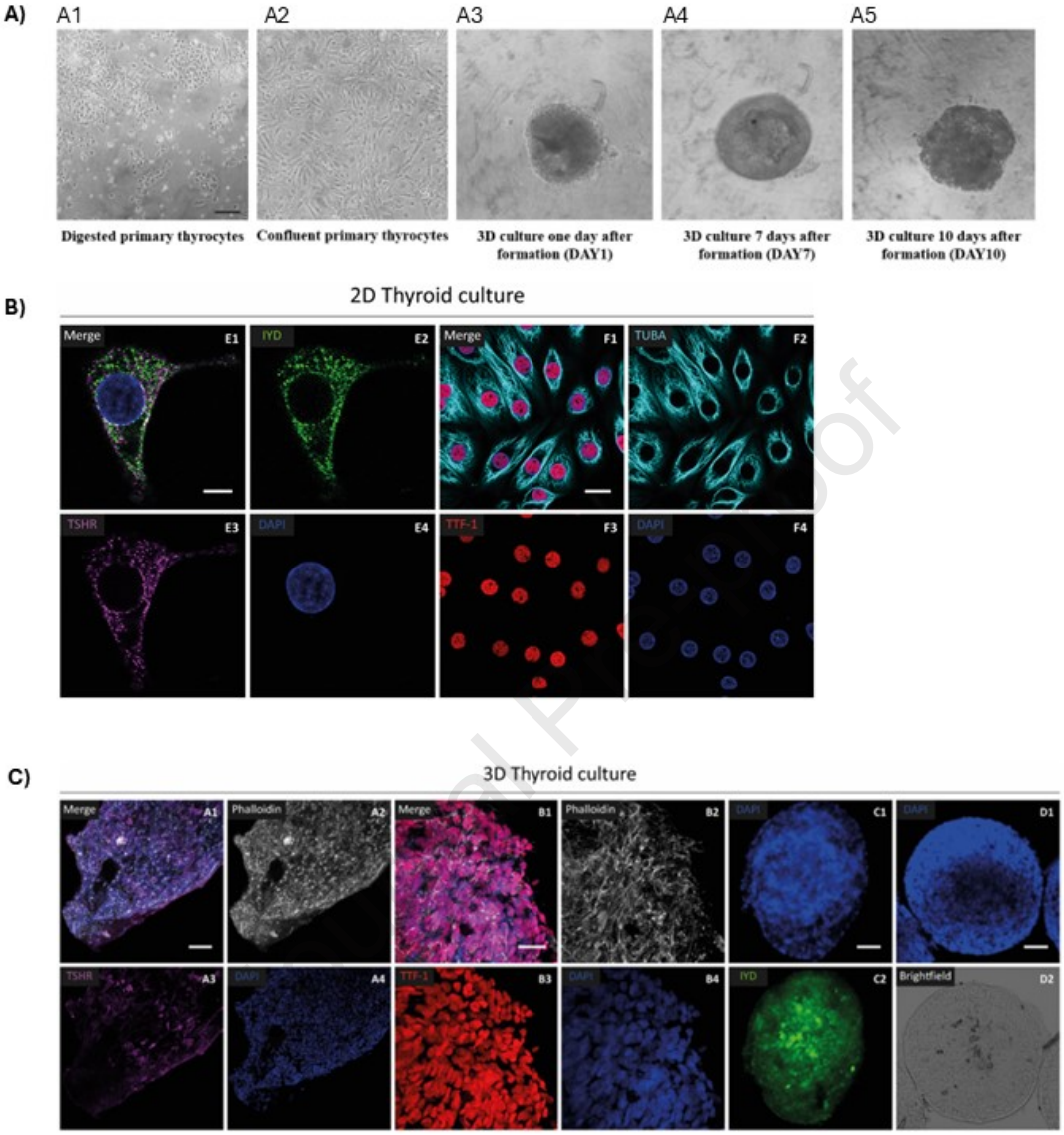
A)
A1
A2
A3
A4
A5
Digested primary thyrocytes
Confluent primary thyrocytes
3D culture one day after formation (DAY1)
3D culture 7 days after formation (DAY7)
3D culture 10 days after formation (DAY10)
B)
2D Thyroid culture
Merge
E1
IYD
E2
Merge
F1
TUBA
F2
TSHR
E3
DAPI
E4
TTF-1
F3
DAPI
F4
C)
3D Thyroid culture
Merge
A1
Phalloidin
A2
Merge
B1
Phalloidin
B2
DAPI
C1
DAPI
D1
TSHR
A3
DAPI
A4
TTF-1
B3
DAPI
B4
IYD
C2
Brightfield
D2

Journal Pre-proof

Journal Pre-proof

Figure 2

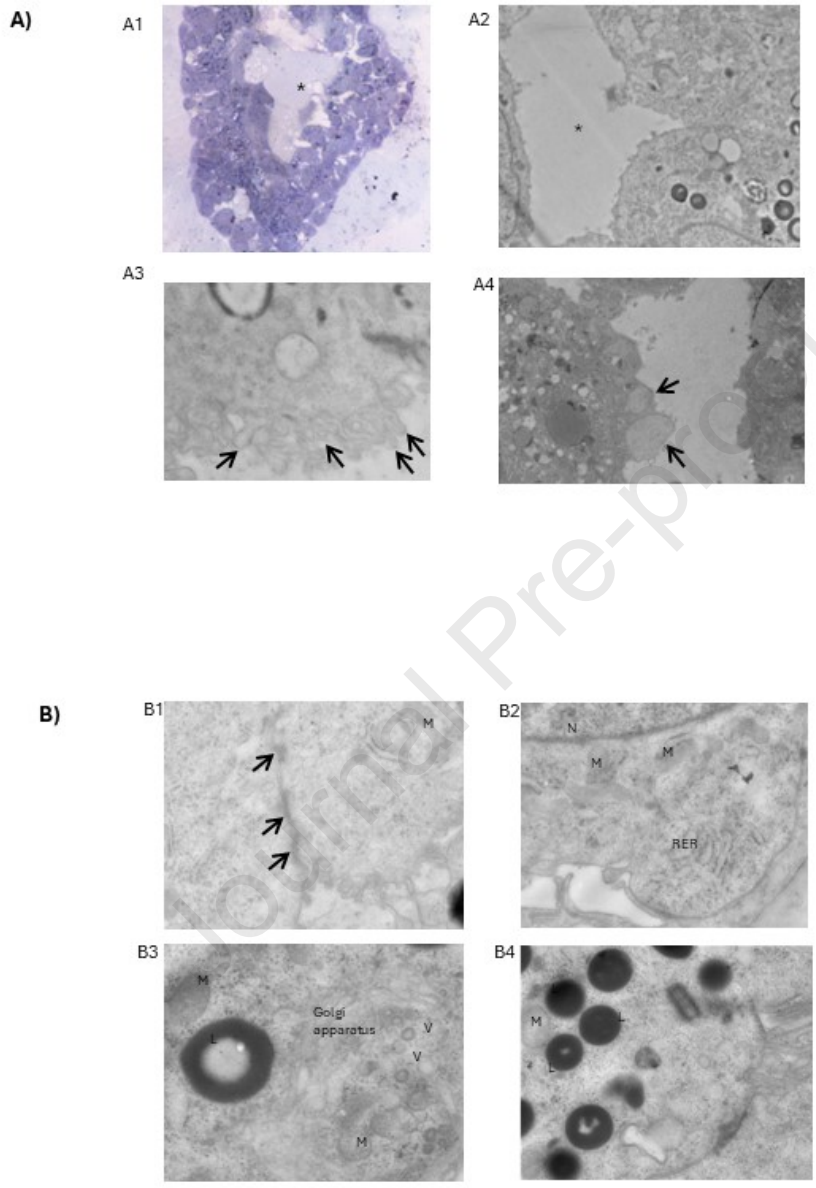

Journal Pre-proof

Journal Pre-proof

Journal Pre-proof

Figure 3

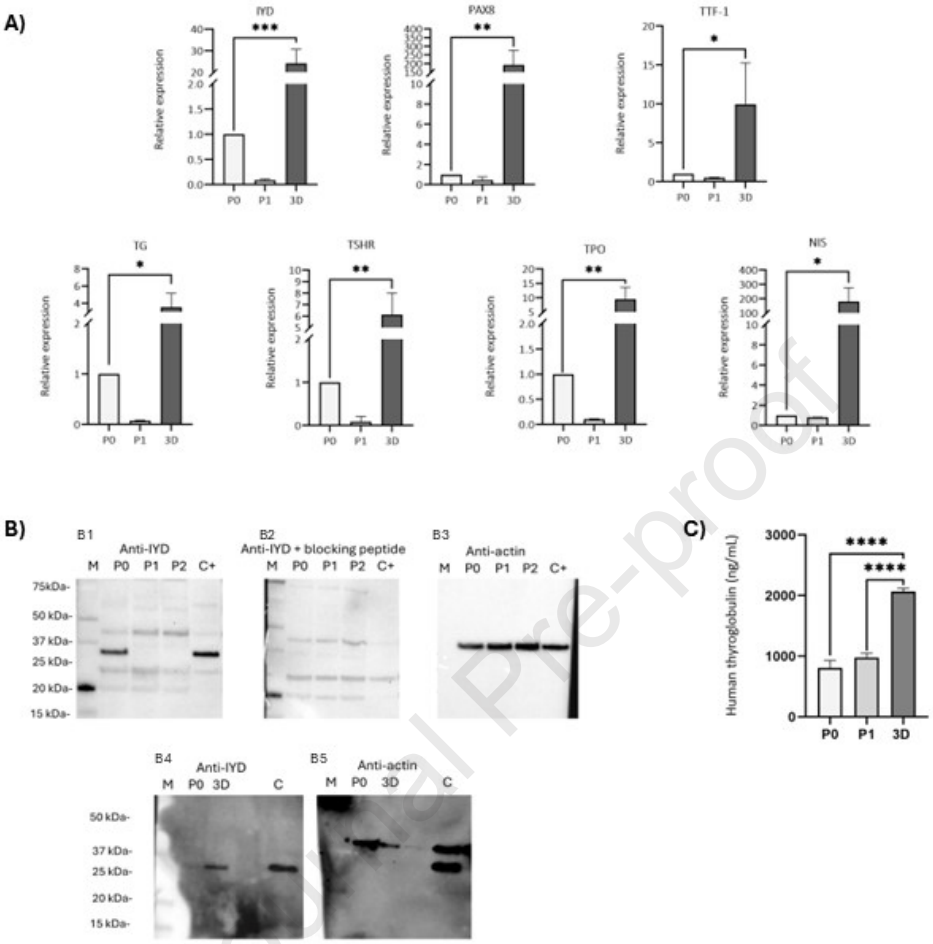

Journal Pre-proof

Journal Pre-proof

Journal Pre-proof

Figure 4

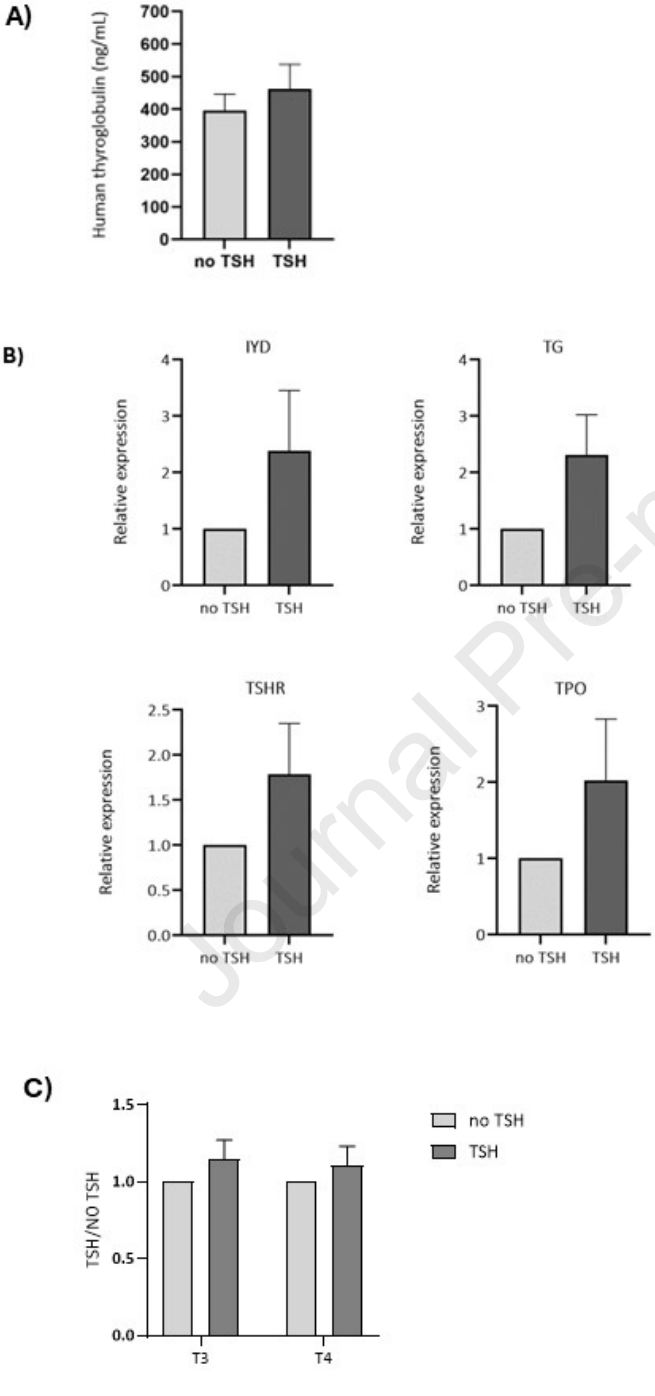

Journal Pre-proof

Journal Pre-proof

Journal Pre-proof

Figure 5

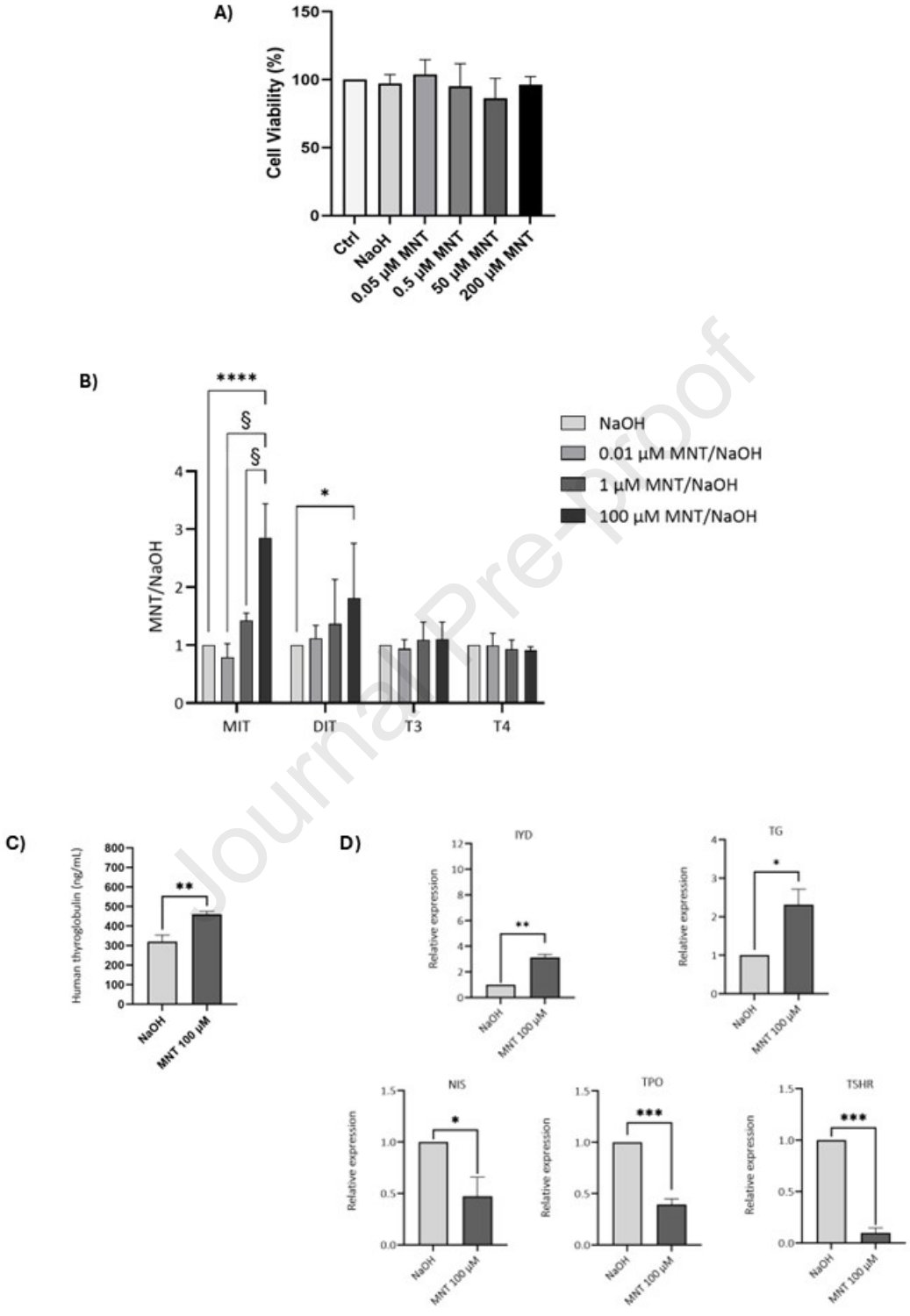

Journal Pre-proof

Highlights

- Enhanced marker expression in 3D cultures reveals organoid model fidelity.
- 3D thyroid cultures are valuable for studying metabolism and disorders.
- Organoid-based thyroid model offers insight into endocrine disruptors.
- Thyroid organoids provide ethical research avenues for studying gland function.

Journal Pre-proof

Journal Pre-proof

Declaration of interests

☒ The authors declare that they have no known competing financial interests or personal relationships that could have appeared to influence the work reported in this paper.

☐ The authors declare the following financial interests/personal relationships which may be considered as potential competing interests:

Journal Pre-proof